Journal of Photochemistry & Photobiology, A: Chemistry 456 (2024) 115849

Contents lists available at ScienceDirect

Journal of Photochemistry & Photobiology, A: Chemistry

journal homepage: www.elsevier.com/locate/jphotochem

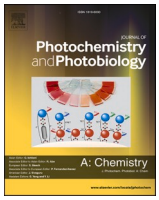

Cationic thiazolothiazole derivatives – A new class of photosensitizing agents against *Staphylococcus aureus*

Ana F.R. Cerqueira [a,1], María E. Pérez [b,1], Natalia S. Gsponer [b,1], Maria G.P.M.S. Neves [a], A. Jorge Parola [c], Edgardo N. Durantini [b,*], Augusto C. Tomé [a,*]

[a] LAQV-REQUIMTE, Department of Chemistry, University of Aveiro, 3810-193 Aveiro, Portugal
[b] IDAS-CONICET, Departamento de Química, Facultad de Ciencias Exactas, Físico-Químicas y Naturales, Universidad Nacional de Río Cuarto, Ruta Nacional 36 Km 601, X5804BYA Río Cuarto, Córdoba, Argentina
[c] LAQV-REQUIMTE, Department of Chemistry, NOVA School of Science and Technology, FCT NOVA, Universidade NOVA de Lisboa, 2829-516 Caparica, Portugal

ARTICLE INFO

Keywords:
Thiazolothiazole
Photosensitizer
Photoinactivation
Microorganism
Biofilm

ABSTRACT

The assessment of thiazolothiazoles (TzTz) as photosensitizers in photodynamic inactivation (PDI) experiments is reported for the first time. Mono and dicationic TzTz derivatives were synthesized, and their photosensitizing ability was assessed on *Staphylococcus aureus* cells, both in suspension or attached to a surface, and using white light. The biological results showed that the photodynamic efficiency of these derivatives is dependent on the TzTz structure and irradiation time. The best results were obtained with the monocationic derivative **TPATzTzPyMe**$^{+}$ that allowed to reach a value over 7 log (99.9999 %) cell inactivation after white light irradiation for 30 min. Furthermore, **TPATzTzPyMe**$^{+}$ also revealed to be effective on the inactivation of *S. aureus* adhered to surfaces, a good indication of its potential to prevent biofilm formation. **TPATzTzPyMe**$^{+}$ was also effective against *Escherichia coli*, with a reduction in cell viability of 5.7 log after irradiation for 30 min.

1. Introduction

Due to the widespread use of antibiotics, there is an increasing need to develop effective and safe antimicrobials that can replace or complement traditional antibiotics in combating drug-resistant bacteria [1]. Photodynamic inactivation (PDI), also known as antimicrobial photodynamic therapy (aPDT), emerged as an alternative solution against multidrug resistant microorganisms [2]. This is a non-invasive technique that requires a nontoxic photosensitizer (PS), light (white light or visible light with a specific wavelength) and dioxygen ($^{3}O_2$). After the administration and irradiation of the PS, cytotoxic and reactive oxygen species (ROS), mainly singlet oxygen ($^{1}O_2$), are generated leading, after their interaction with vital biomolecules, to the inactivation of the microorganisms. This process has been used to effectively inactivate bacteria, virus, and fungi [3–6].

Extensive research has been dedicated to explore the potential of a range of small molecules [7,8] as phototherapeutic agents in the inactivation of bacteria, such as porphyrins, chlorins, bacteriochlorins, and phthalocyanines [9–12], BODIPYs [13], cyanine dyes [14], phenothiazines and xanthenes [15], and diketopyrrolopyrroles [16,17].

Thiazolo[5,4-*d*]thiazoles, also known as thiazolothiazoles (TzTz), constitute a class of heterocyclic compounds characterized by a rigid coplanar fused bicyclic scaffold with an extended π-conjugation system. These compounds are attractive candidates for different applications [18–21]. In fact, TzTz compounds have already been successfully employed as probes for live-cell imaging [22–25], components in solar cells devices [26–32], organic light-emitting diodes (OLEDs) [33], fluorescent metal–organic frameworks (MOFs) [23,34–36], chemosensors [25,36–39], and photocatalysts [40,41]. Surprisingly, only one study concerning the evaluation of TzTz as potential therapeutic agents was reported [42]. In that article, a symmetrical and a non-symmetrical TzTz derivatives bearing catechol units were evaluated as inhibitors of the human 5-lipoxygenase (5-hLOX), that is involved in a variety of inflammation-related diseases, and as antibacterials against *Staphylococcus aureus*. The results showed that both TzTz were less efficient, or inactive, as 5-hLOX inhibitors and as antibacterials than similar 1,3-thiazole derivatives. Furthermore, in the context of this work, it is important to highlight that in the cited study, the inactivation of *S. aureus* was

* Corresponding authors.
E-mail address: actome@ua.pt (A.C. Tomé).
[1] These authors contributed equally to this work.

https://doi.org/10.1016/j.jphotochem.2024.115849
Received 19 February 2024; Received in revised form 22 May 2024; Accepted 19 June 2024
Available online 24 June 2024

carried without light irradiation. In fact, as far as we know, until now, TzTz have never been used as PS in PDT or PDI experiments.

In this paper, we present the synthesis and characterization of six cationic TzTz derivatives (*vide infra* Fig. 1), highlighting their photophysical properties. Moreover, we investigate their potential as photosensitizing agents against *S. aureus*, aiming to find new lead compounds for antimicrobial applications.

2. Experimental section

2.1. Materials and methods

The experimental details for the synthesis of the cationic TzTz are reported in the Supplementary Material.

2.2. Singlet oxygen generation

The capability of the cationic TzTz to generate singlet oxygen was evaluated by monitoring the photooxidation of 9,10-dimethylanthracene (DMA), a singlet oxygen quencher. Solutions of each compound presented in Fig. 1 (**Br_2TPATzTzPyMe$^+$**, **Br_2TPATzTzPyPent$^+$**, **TPATzTzPyMe$^+$**, **TzTz(PyMe)$_2^{2+}$**, **TzTz(PyPent)$_2^{2+}$**, **TzTz(PyDodec)$_2^{2+}$**) and 5,10,15,20-tetraphenylporphyrin (**TPP**) ($\Phi_\Delta = 0.65$) [43,44] in dimethylformamide (DMF) (2.5 mL) were prepared in quartz cells ($Abs_{420} \approx 0.1$). Subsequently, a 30 μM solution of DMA in DMF was added and the resulting solutions were irradiated with monochromatic light (λ = 420 nm). The absorbance decay of DMA at 378 nm was measured at intervals of 60 s over a period of 900 s and the results were registered in a first-order plot. The kinetics of DMA photooxidation in DMF, in the absence of any PS, was also assessed and no significant photodegradation was observed under the same irradiation conditions.

2.3. Bacterial strain cultures

Methicillin-resistant *S. aureus* (ATCC 43300) cells were aerobically cultured overnight at 37 °C in tryptic soy (TS) broth (4 mL) under sterile conditions [45]. Subsequently, 50 mL of this culture was aseptically transferred to fresh TS broth (4 mL) and incubated at 37 °C until reaching the mid-logarithmic phase of growth ($Abs_{660} = 0.6$). Then, the *S. aureus* cells were harvested through centrifugation at 3000 rpm for 15 min and suspended in a 4 mL solution of 10 mM phosphate-buffered saline (PBS, pH 7.2). This process resulted in a cell density of approximately 10^8 colony forming units (CFU)/mL. The viability of *S. aureus* cells was assessed using the spread plate method in triplicate. The CFU count was determined on TS agar plates after an incubation period of around 24 h at 37 °C in the dark. *Escherichia coli* (ATCC 25922) cells were cultured as previously described [46].

2.4. Photoinactivation of S. aureus cell suspensions

S. aureus suspensions (2 mL, ~10^8 CFU/mL) in PBS were treated with 2 μM TzTz (10 μL) for 15 min in the dark at 37 °C in 13x100 mm Pyrex culture tubes [47]. The application of these compounds was carried out using a 0.4 mM stock solution in DMF. Then, 200 μL of cell suspensions were distributed into 96-well microtiter plates, and the cultures were subjected to irradiation for 5, 15, and 30 min using a Novamat 130 AF projector (Braun Photo Technik, Nürnberg, Germany) equipped with a 150 W lamp. Optical filters were utilized to define a wavelength range between 350 and 800 nm. The projector was positioned vertically with the light beam focused onto the lid of the 96-well microtiter plate. This arrangement produced a fluence rate of 90 mW/cm^2 (Radiometer Laser Mate-Q, Coherent, Santa Clara, CA, USA) [46]. Quantification of viable bacterial cells was performed following the procedure described above [45].

2.5. Photoinactivation of S. aureus at the single-bacterium level

Fluorescence microscopy analyses were conducted following a previously established methodology with slight adjustments, utilizing an inverted fluorescence microscope (BIM500FL, Bioimager, ON, Canada) [48]. *S. aureus* cells were cultivated aerobically on TS agar overnight at 37 °C. Subsequently, a single colony was selected and cultured overnight in TS agar. Bacterial specimens were harvested from the agar by adding 1 mL of PBS and removing the agar streaks. Then, a suspension of *S. aureus* (1 mL) was incubated for 30 min at 37 °C within a chamber constructed from a polymeric cylinder affixed to a coverslip. During this process, bacterial cells were adhered to the glass surface while any unbound bacteria were eliminated from the chamber by washing with PBS. The experimental steps involved the addition of PBS (583 μL) and propidium iodide (PI) (1 μM, 5 μL from a 120 mM stock solution in DMSO/water (1:9)) to the cells fixed on the glass surface within the chamber. Subsequently, the cells were incubated for 15 min at 37 °C in the dark. After that, the bacteria were treated with 2 μM TzTz (12 μL from a 1x10^{-4} M stock solution in DMF), and the cultures were further incubated for another 15 min at 37 °C in the dark. For photoinactivation tests, the chamber was irradiated with a Cole-Parmer illuminator containing 150 W halogen lamp (41720 series, Cole-Parmer, Vernon Hills, IL) using an optical fiber. This setup yielded a light fluence rate of 6.6 mW/cm^2. The samples were exposed to irradiation for 5, 15 and 30 min. To detect dead cells, PI was excited with green light through a bandpass filter (515/35). Fluorescence images of PI were captured using an emission bandpass filter (645/75). Additionally, a brightfield image was acquired to verify the presence of bacterial cells. Bioimages were acquired using a 100 × magnification objective using a CMOS camera. Images were processed with FIJI-ImageJ program.

2.6. Controls and statistical analysis

Irradiated controls of *S. aureus* cultures were performed using cell suspensions (~10^8 CFU/mL) in 2 mL of PBS without the addition of TzTz. Dark controls were conducted on cell suspensions incubated with 2 μM TzTz for 15 min in the absence of light at 37 °C, and they were subsequently kept under these conditions for 5, 15, and 30 min. Each value denotes the mean of three separate experiments with its standard

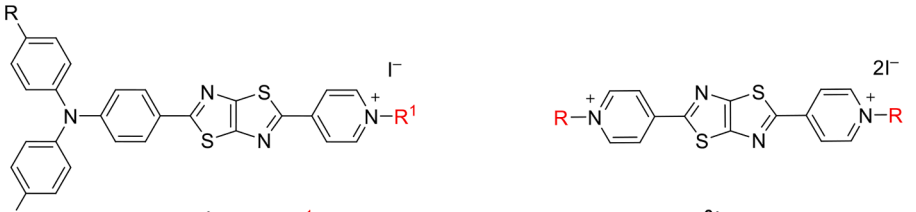

TPATzTzPyMe$^+$, R = H, R^1 = Me
Br_2TPATzTzPyMe$^+$, R = Br, R^1 = Me
Br_2TPATzTzPyPent$^+$, R = Br, R^1 = $(CH_2)_4CH_3$

TzTz(PyMe)$_2^{2+}$, R = Me
TzTz(PyPent)$_2^{2+}$, R = $(CH_2)_4CH_3$
TzTz(PyDodec)$_2^{2+}$, R = $(CH_2)_{11}CH_3$

Fig. 1. Structures of the mono and dicationic TzTz derivatives.

deviation. The significance of the differences between the means was analyzed using one-way ANOVA with a confidence level of 95 % ($p < 0.05$) [47].

3. Results and discussion

3.1. Synthesis

The cationic TzTz derivatives used in this work (Fig. 1) were synthesized in two steps. Firstly, the neutral TzTz derivatives were obtained from the reaction of dithiooxamide with pyridine-4-carbaldehyde and 4-(diphenylamino)benzaldehyde or 4-[bis(4-bromophenyl)amino]benzaldehyde in anhydrous DMF at 130 °C, as illustrated in Scheme S1. This allowed us to prepare one symmetrical (with two pyridyl groups) and two non-symmetrical (with a triphenylamino unit and a pyridyl group) TzTz derivatives. The structures of compounds **TzTzPy$_2$**, **(TPA)$_2$TzTz**, **(Br$_2$TPA)$_2$TzTz** and **TPATzTzPy** (see SI) were confirmed by comparing their spectral data with those reported in the literature [24,49–51]. The structure of compound **Br$_2$TPATzTzPy** was confirmed by its ^{1}H NMR, ^{13}C NMR and MS spectra (see SI).

The last step of the synthesis was the quaternization of the pyridyl groups with methyl iodide, 1-iodopentane or 1-iodododecane. These reactions were carried out in anhydrous DMF at 40 °C. The structures of all derivatives were confirmed by ^{1}H NMR, ^{13}C NMR and MS spectra (see SI). The presence of the signals corresponding to the resonances of the protons of the *N*-alkyl groups on the ^{1}H NMR spectra is a clear evidence that the cationization occurred. For example, in the ^{1}H NMR spectrum of **TPATzTzPyMe$^+$** (Fig. S6), an additional singlet appeared at 4.36 ppm, corresponding to the protons of the methyl group, when compared to the neutral precursor. The MS spectra of the monocationic TzTz derivatives showed the base peak corresponding to $[M - I^-]^+$, while for the dicationic derivatives the base peak corresponds to $[M - 2I^-]^{2+}$.

3.2. Photophysical properties

The absorption and emission spectra of TzTz are presented in Figs. 2 and 3 and their photophysical properties are summarized in Table 1. The absorption spectrum of the neutral **Br$_2$TPATzTzPy** displays a band centered at 417 nm and a band of minor intensity at 315 nm. The UV–Vis spectra of **Br$_2$TPATzTzPyMe$^+$** and **Br$_2$TPATzTzPyPent$^+$** showed a red shift of 26 nm and 46 nm for the first absorption band and of 57 nm and 58 nm for the second absorption band, respectively, relatively to the spectrum of the neutral TzTz. Concerning the spectrum of **TPATzTzPyMe$^+$**, it showed a strong band at 485 nm and a minor one at 352 nm. In the case of the dicationic TzTz, the UV–Vis spectrum of each derivative showed a band at ca. 390 nm, with a red shift of *ca.* 40 nm when compared with the neutral derivative **TzTzPy$_2$** (λ_{max} 350 nm) [52].

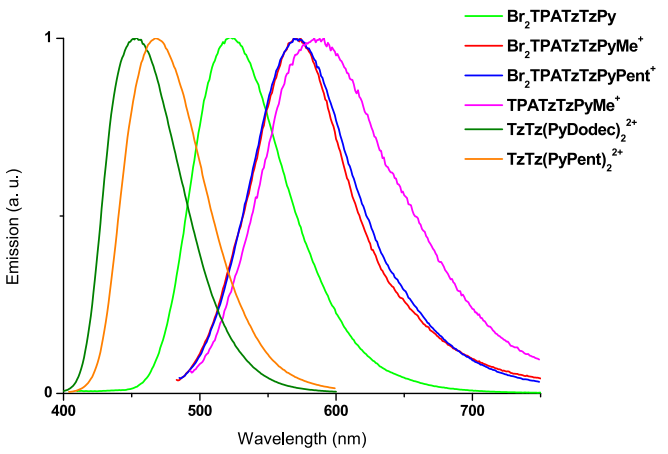

Fig. 3. Normalized emission spectra of TzTz derivatives in DMF.

The emission spectra of non-symmetrical cationic TzTz showed a maximum emission wavelength between 558 and 569 nm. **Br$_2$TPATzTzMe$^+$** and **Br$_2$TPATzTzPent$^+$** showed a bathochromic shift of 53 nm and 49 nm, respectively, relative to the emission band of the neutral **Br$_2$TPATzTzPy** derivative (λ_{max} 520 nm). The dicationic TzTz showed the maximum emission wavelength between 453 and 468 nm. All TzTz derivatives exhibit Stokes shifts in the range 3241–4750 cm^{-1}, which is consistent with previously reported data [24,53].

3.3. Photooxidation of DMA

The capacity of cationic TzTz to generate $^1O_2$ upon irradiation was assessed by an indirect method based on the absorption decay of a DMA solution. The samples were irradiated at 420 nm under aerobic conditions and the photooxidation of DMA was monitored by the decrease of

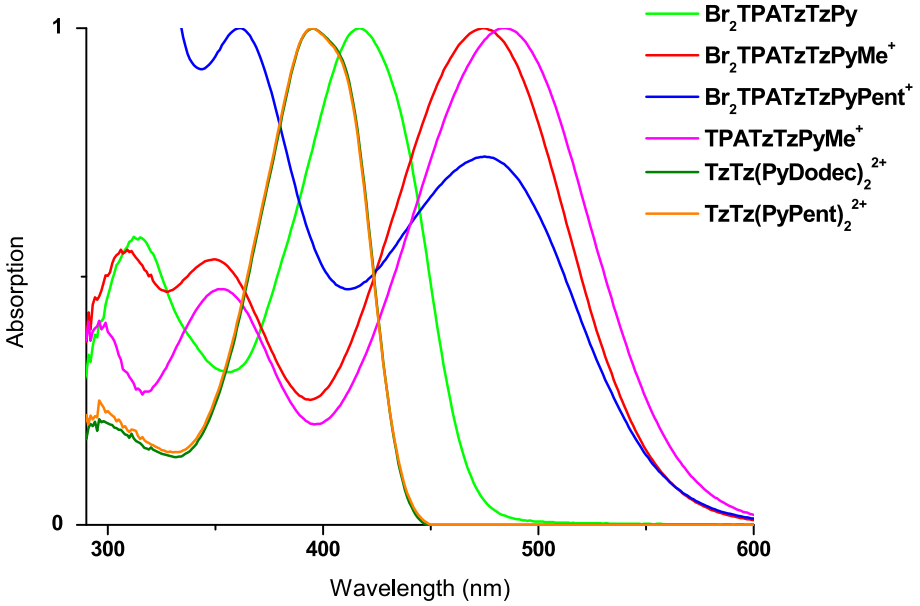

Fig. 2. Normalized absorption spectra of TzTz derivatives in DMF.

Table 1
Absorption and emission data of TzTz derivatives.

TzTz	$\lambda_{max,abs}$ (nm)	log ε (M^{-1} cm^{-1})	$\lambda_{max,em}$ (nm)	Stokes shift (nm)[c]	(cm^{-1})[c]	Φ_F	Φ_Δ
Br_2TPATzTzPy[a]	315	4.42	520	103	4750	0.60[d]	n.d.
	417	4.66					
Br_2TPATzTzPyMe^{+} [b]	309	4.26	573	99	3645	0.04[d]	0.014
	349	4.24					
	474	4.51					
Br_2TPATzTzPyPent^{+} [b]	361	3.77	569	94	3478	0.07[d]	0.041
	475	3.64					
TPATzTzPyMe^{+} [b]	352	4.43	584	99	3496	0.14[d]	0.018
	485	4.76					
TzTz(PyMe)$_2^{2+}$ [b]	392	4.50	454	62	3484	0.91[e]	0.086
TzTz(PyPent)$_2^{2+}$ [b]	395	4.66	468	73	3948	0.74[e]	0.110
TzTz(PyDodec)$_2^{2+}$ [b]	395	4.46	453	58	3241	0.20[e]	0.030

[a] 10^{-5} mol.L^{-1} in $CHCl_3$. [b] 10^{-5} mol.L^{-1} in DMF. [c] Stokes shift was calculated as the difference (in wavenumbers) between the maximum of the first absorption band and the maximum of the fluorescence spectrum [54].
[d] Excitation at 400 nm; calculated using 2-[4-(diphenylamino)phenyl]-5-(4-pyridyl)thiazolo[5,4-*d*]thiazole as fluorescence standard ($\Phi_F = 0.54$ in $CHCl_3$) [24].
[e] Excitation at 380 nm; calculated using 2,5-bis(1-methylpyridin-1-ium-4-yl)thiazolo[5,4-*d*]thiazole (**TzTz(PyMe)$_2^{2+}$**) as fluorescence standard ($\Phi_F = 0.92$ in H_2O) [55].

the absorbance at $\lambda_{max} = 378$ nm (Fig. S31). The Φ_Δ values found for all TzTz derivatives are summarized in Table 1. These values are much lower than the Φ_Δ value for **TPP** ($\Phi_\Delta = 0.65$ in DMF) [43,44]. While low values for Φ_Δ could be expected for TzTz derivatives with high Φ_F (observed for the symmetric derivatives **TzTz(PyMe)$_2^{2+}$** and **TzTz(PyPent)$_2^{2+}$**), there is no clear correlation in the overall results, indicating the presence of other deactivation processes of the excited state. Moreover, the derivative with the highest antimicrobial activity (**TPATzTzPyMe^{+}**) shows low Φ_Δ and low Φ_F values. This suggests that photobactericidal mechanisms other than those involving the production of $^1O_2$, such as the generation of superoxide radical, $O_2^{\bullet-}$, upon electron transfer, and photothermal effect, arising from internal conversion, may be operative.

3.4. Photoinactivation of *S. aureus* cell suspensions

Photoinactivation induced by TzTz was conducted on in *S. aureus* cell suspensions, using a cell density of ~10^8 CFU/mL. This microbial strain was selected due to its potential to cause pathogenic diseases in humans [56]. Microorganism cultures suspended in PBS were treated with 2 μM TzTz for 15 min at 37 °C in the dark. This concentration was selected based on previous results of photosensitizers with photodynamic properties similar to TzTz derivatives [17]. Subsequently, the cells were exposed for 5, 15 and 30 min to white light. It was observed that at this concentration, TzTz did not exhibit toxicity to the microbial cells during a 30 min incubation in the dark (Fig. 4). Additionally, the viability of bacteria remained unaffected by cell irradiation in the absence of TzTz (Fig. 5). Consequently, the PDI of cultures observed after irradiating *S. aureus* cells treated with TzTz was attributed to the photodynamic activity sensitized by these compounds. The survival of microbial cells following different PDI treatments is depicted in Fig. 5. Cell viability was influenced by both the TzTz derivative and the period of exposure to white light. After 30 min of irradiation, 1 log decrease in bacterial survival was found in *S. aureus* cells treated with **Br_2TPATzTzPyPent^{+}**, **TzTz(PyMe)$_2^{2+}$**, and **TzTz(PyPent)$_2^{2+}$**. Additionally, **TzTz(PyDodec)$_2^{2+}$** and **Br_2TPATzTzPyMe^{+}** demonstrated a photoinactivation resulting in 2 log (99 %) and 3 log (99.9 %) reduction, respectively, after the same duration of irradiation. However, the photokilling capacity induced by **TPATzTzPyMe^{+}** was higher, reaching a 3.5 log decrease in cell survival upon 5 min of irradiation. In addition, it was able to eliminate the bacteria, which signifies over 7 log cell inactivation, by irradiation of the *S. aureus* cells treated with this TzTz derivative for 30 min. This reduction in viability produced by **TPATzTzPyMe^{+}** represented a value greater than 99.9999 % of cell inactivation. Based on these findings, the phototoxic activity of **TPATzTzPyMe^{+}** was also examined against the Gram-negative bacteria *E. coli*. The survival of *E. coli* cells after different treatment periods are shown in Fig. 6. After 30 min of irradiation, this PS caused a reduction in cell viability of 5.7 log units. This is an interesting finding because **TPATzTzPyMe^{+}** demonstrated effectiveness not only in

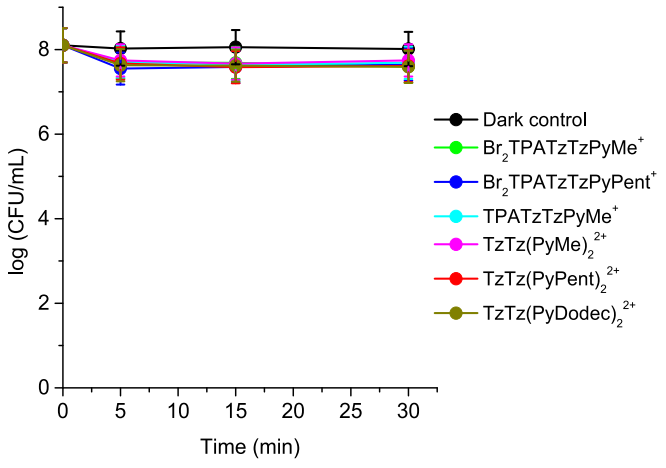

Fig. 4. Survival of *S. aureus* (~10^8 CFU/mL) treated with 2 μM TzTz for 15 min at 37 °C in the dark and kept in the dark for different times.

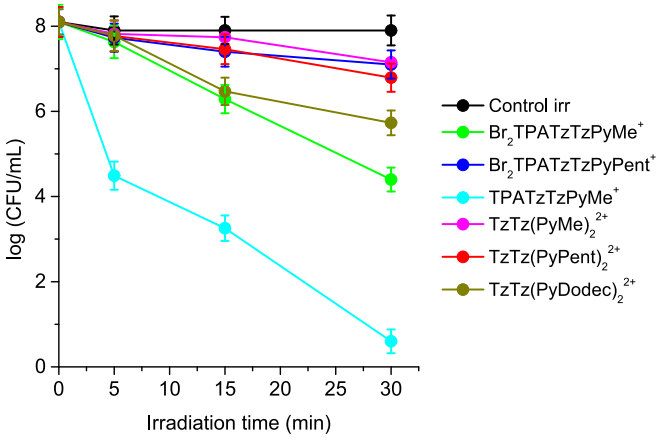

Fig. 5. Survival of *S. aureus* (~10^8 CFU/mL) treated with 2 μM TzTz for 15 min at 37 °C in the dark and then irradiated with white light (90 mW/cm^2) for 5, 15 and 30 min. Irradiated control: culture without TzTz but irradiated with white light (90 mW/cm^2).

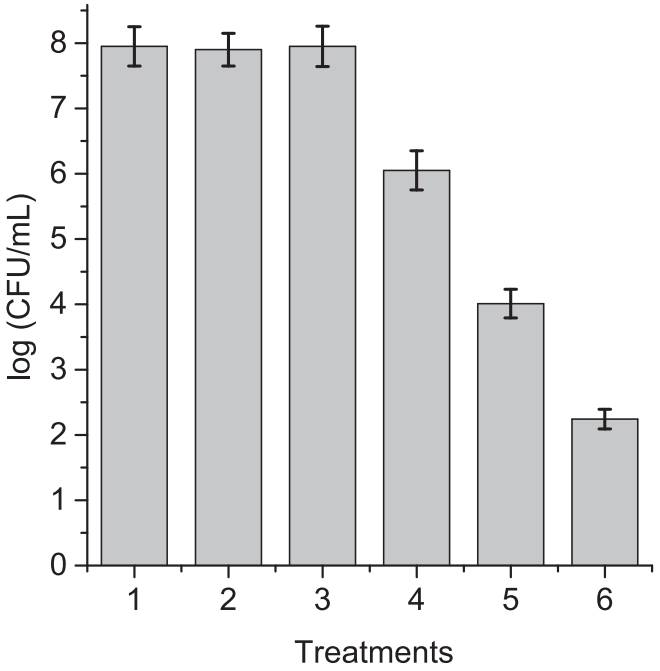

Fig. 6. Survival of *E. coli* (~10^8 CFU/mL) treated with 2 μM **TPATzTzPyMe$^+$** for 15 min at 37 °C in the dark and then irradiated with white light (90 mW/cm^2) for different periods, (1) cells in the dark, (2) irradiated cells for 30 min, (3) cells + PS in the dark for 30 min, (4) irradiated cells + PS for 5 min, (5) irradiated cells + PS for 15 min, (6) irradiated cells + PS for 30 min.

inactivating *S. aureus* but also in eliminating *E. coli* with 99.999 % efficiency.

The photobleaching of compounds **TPATzTzPyMe$^+$** and **Br$_2$TPATzTzPyMe$^+$**, which were the most effective in eradicating bacteria, were measured under conditions similar to those used to photoinactivate *S. aureus* (Fig. S32). From the first-order plots (Fig S33), the photobleaching half-life times ($\tau_{1/2}$) of **TPATzTzPyMe$^+$** and **Br$_2$TPATzTzPyMe$^+$** were 18 and 27 min, respectively.

The remaining TzTz do not apparently interact with bacteria and therefore did not present any band in cell suspensions, neither absorption nor fluorescence, to be able to monitor photobleaching over time. The remaining TzTz did not appear to interact with the bacteria. Therefore, no absorption or fluorescence bands were detected in the cell suspensions, precluding the monitoring of photobleaching over time. The results indicate that the compounds **TPATzTzPyMe$^+$** and **Br$_2$TPATzTzPyMe$^+$** can effectively interact with bacterial cells, increasing their efficiency to eradicate *S. aureus*.

3.5. Photoinactivation of S. aureus attached to surfaces

PDI sensitized by TzTz was also determined by observing individual bacteria under a fluorescence microscope. To achieve this, *S. aureus* cells were affixed to the surface of a coverslip within a circular chamber, following the previously outlined procedure [48]. This method relies on the presence of bacterial hairs that facilitate the adherence of *S. aureus* cells to glass surfaces [57]. Fluorescence images were compared with phase-contrast photographs to confirm the presence and position of the bacterial cells on the surfaces (Fig. 7). The process involved treating individual *S. aureus* cells with 1 μM PI for 15 min. Subsequently, the bacteria were incubated with 2 μM TzTz in PBS for an additional 15 min in the absence of light. In this procedure, PI served as a fluorophore to detect cell death of attached bacteria inside the chamber [58]. In this procedure, light irradiation from an optical fiber was applied to *S. aureus* cells for varying durations. These tests were conducted using the two most potent TzTz derivatives (**Br$_2$TPATzTzPyMe$^+$** and **TPATzTzPyMe$^+$**) for photoinactivating bacterial suspensions. The progression of TzTz-sensitized PDI and control outcomes is illustrated in Fig. 7, covering irradiation times from 0 to 30 min. Control experiments involving cells irradiated without TzTz exhibited negligible cell damage after a 30 min of irradiation (Fig. 7, last row). In the presence of TzTz,

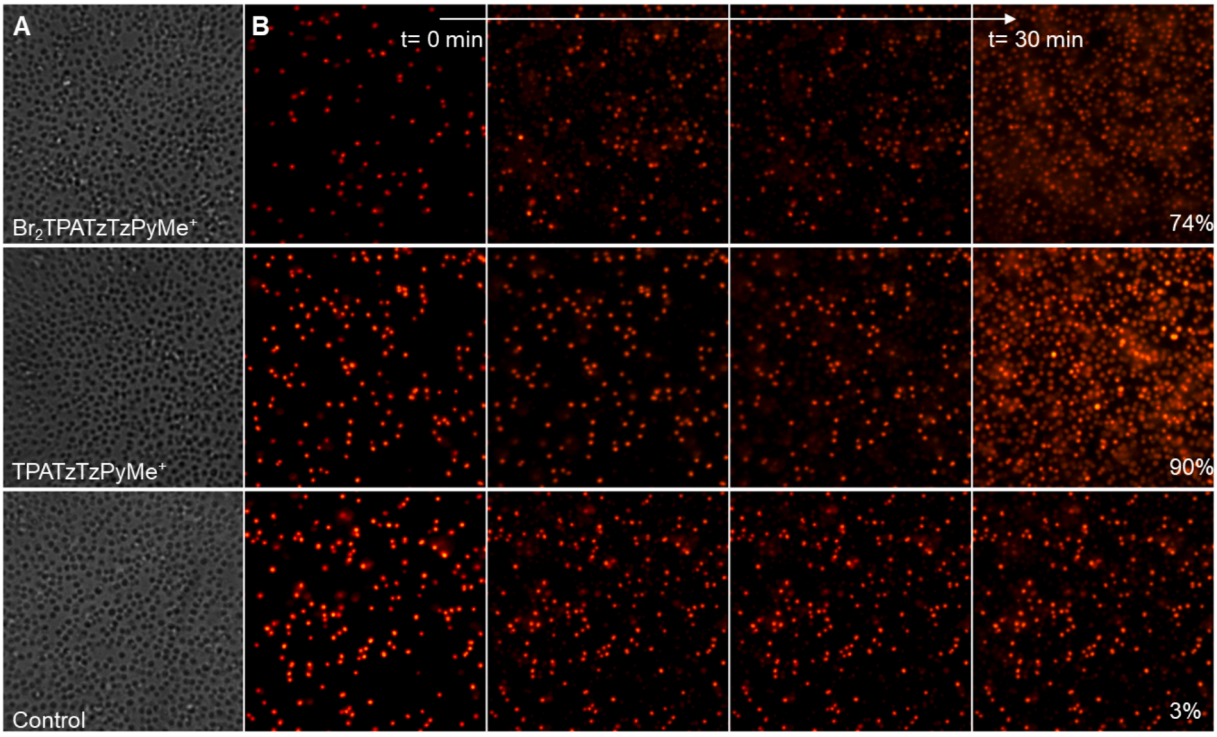

Fig. 7. Microscopy images of *S. aureus* incubated with 2 μM TzTz for 15 min in the dark and irradiated with white light (6.6 mW/cm^2) for different times (0, 5, 15, and 30 min); column A: cells under bright field; columns B: fluorescence emission of PI.

photodamage of *S. aureus* cells was evidenced through an increase in red fluorescence, a characteristic indicative of cell death. **Br_2TPATzTzPyMe$^+$** demonstrated approximately 74 % inactivation of *S. aureus* cells (Fig. 6, first row). As found in the tests with cell suspensions in PBS, **TPATzTzPyMe$^+$** was the most effective PS for eliminating surface-adhering *S. aureus* cells. The photodynamic action induced by this TzTz derivative achieved an inactivation exceeding 90 % after 30 min of irradiation (Fig. 7, second row). Consequently, these findings highlight **TPATzTzPyMe$^+$** as an effective compound in the photoinactivation of *S. aureus* cells at the individual bacterium level, representing a simplified model of the initial stage in biofilm formation [59].

4. Conclusions

Symmetrical and non-symmetrical TzTz derivatives bearing one or two 4-pyridyl groups were synthesized and the pyridyl groups were then quaternized with methyl iodide, 1-iodopentane or 1-iodododecane to afford the corresponding mono and dicationic derivatives. The photosensitizing ability of the cationic TzTz was assessed on *S. aureus* cells and the results showed that monocationic derivatives were more efficient PS for the inactivation of the bacterium than the dicationic ones. The best results for the PDI experiments (carried using 2 μM TzTz and white light with a fluence rate of 90 mW/cm^2) were obtained with the monocationic derivative **TPATzTzPyMe$^+$** that allowed to reach a value over 7 log cell inactivation after irradiation for 30 min. This reduction in viability of *S. aureus* induced by **TPATzTzPyMe$^+$** represents a value greater than 99.9999 % of cell inactivation. Furthermore, this TzTz derivative was also effective for the photoinactivation of *S. aureus* cells attached to a surface, a good indication that it can be used for the inactivation of biofilms. As a final remark, the results of this work clearly indicate that cationic TzTz derivatives can be considered a new class of photosensitizers for PDI. **TPATzTzPyMe$^+$**, in particular, should be considered a new lead compound worth optimizing for antimicrobial applications.

5. Authors statement

The authors declare that the submitted manuscript is original, has not been published before and is not currently being considered for publication elsewhere.

Authors also confirm that the manuscript has been read and approved by all named authors.

Funding

This work received financial support from PT national funds (FCT/MCTES, Fundação para a Ciência e a Tecnologia and Ministério da Ciência, Tecnologia e Ensino Superior) for LAQV-REQUIMTE through the projects UIDB/50006/2020 and UIDP/50006/2020, and ANPCYT-FONCYT Argentina (PICT 02391/19).

CRediT authorship contribution statement

Ana F.R. Cerqueira: Investigation, Data curation, Writing – original draft. **María E. Pérez:** Investigation, Data curation, Writing – original draft. **Natalia S. Gsponer:** Writing – original draft, Investigation, Data curation. **Maria G.P.M.S. Neves:** Supervision, Writing – review & editing. **A. Jorge Parola:** Writing – review & editing, Supervision. **Edgardo N. Durantini:** Writing – review & editing, Supervision, Resources, Methodology, Conceptualization. **Augusto C. Tomé:** Writing – review & editing, Supervision, Resources, Methodology, Conceptualization.

Declaration of competing interest

The authors declare that they have no known competing financial interests or personal relationships that could have appeared to influence the work reported in this paper.

Data availability

No data was used for the research described in the article.

Acknowledgements

Thanks are due to the University of Aveiro and FCT/MCTES for the financial support through PT national funds for LAQV-REQUIMTE (10.54499/LA/P/0008/2020, 10.54499/UIDB/50006/2020 and 10.54499/UIDP/50006/2020), within the PT2020 Partnership Agreement, and to the Portuguese NMR Network. Ana F. R. Cerqueira thanks FCT/MCTES for her doctoral grant (SFRH/BD/135597/2018). N.S.G. and E.N.D. are Scientific Members of CONICET Argentina. M.E.P. thanks CONICET for the research fellowship.

Appendix A. Supplementary data

Supplementary data to this article can be found online at https://doi.org/10.1016/j.jphotochem.2024.115849.

References

[1] B. Aslam, W. Wang, M.I. Arshad, M. Khurshid, S. Muzammil, M.H. Rasool, M. A. Nisar, R.F. Alvi, M.A. Aslam, M.U. Qamar, M.K.F. Salamat, Z. Baloch, Antibiotic resistance: a rundown of a global crisis, Infect. Drug Resist. 11 (2018) 1645–1658, https://doi.org/10.2147/IDR.S173867.
[2] A. Almeida, Photodynamic therapy in the inactivation of microorganisms, Antibiotics 9 (2020) 138, https://doi.org/10.3390/antibiotics9040138.
[3] M.R. Hamblin, Antimicrobial photodynamic inactivation: a bright new technique to kill resistant microbes, Curr. Opin. Microbiol. 33 (2016) 67–73, https://doi.org/10.1016/j.mib.2016.06.008.
[4] C. Vieira, A. Santos, M.Q. Mesquita, A.T.P.C. Gomes, M.G.P.M.S. Neves, M.A. F. Faustino, A. Almeida, Advances in aPDT based on the combination of a porphyrinic formulation with potassium iodide: effectiveness on bacteria and fungi planktonic/biofilm forms and viruses, J. Porphyr. Phthalocyanines. 23 (2019) 534–545, https://doi.org/10.1142/S1088424619500408.
[5] Q. Shi, C. Mou, Z. Xie, M. Zheng, Exploring BODIPY derivatives as photosensitizers for antibacterial photodynamic therapy, Photodiagnosis Photodyn. Ther. 39 (2022) 102901, https://doi.org/10.1016/j.pdpdt.2022.102901.
[6] B. Pucelik, J.M. Dąbrowski, Photodynamic inactivation (PDI) as a promising alternative to current pharmaceuticals for the treatment of resistant microorganisms, Adv. Inorg. Chem. (2022) 65–108, https://doi.org/10.1016/bs.adioch.2021.12.003.
[7] Y. Kong, Q. Jiang, F. Zhang, Y. Yang, Small molecular fluorescent probes: application progress of specific bacteria detection and antibacterial phototherapy, Chem. – an Asian J. 18 (2023) e202300178, https://doi.org/10.1002/asia.202300178.
[8] M. Grimmeisen, C. Jessen-Trefzer, Increasing the selectivity of light-active antimicrobial agents – or how to get a photosensitizer to the desired target, ChemBioChem (2023) e202300177, https://doi.org/10.1002/cbic.202300177.
[9] J. Almeida, G. Zhang, M. Wang, C. Queirós, A.F.R. Cerqueira, A.C. Tomé, G. Barone, M.G.H. Vicente, E. Hey-Hawkins, A.M.G. Silva, M. Rangel, Synthesis, characterization, and cellular investigations of porphyrin– and chlorin–indomethacin conjugates for photodynamic therapy of cancer, Org. Biomol. Chem. 19 (2021) 6501–6512, https://doi.org/10.1039/D1OB01015H.
[10] S.R.D. Gamelas, A.T.P.C. Gomes, M.A.F. Faustino, A.C. Tomé, J.P.C. Tomé, A. Almeida, L.M.O. Lourenço, Photoinactivation of Escherichia coli with water-soluble ammonium-substituted phthalocyanines, ACS Appl. Bio Mater. 3 (2020) 4044–4051, https://doi.org/10.1021/acsabm.0c00128.
[11] M.B. Spesia, E.N. Durantini, Evolution of phthalocyanine structures as photodynamic agents for bacteria inactivation, Chem. Rec. 22 (2022) e202100292, https://doi.org/10.1002/tcr.202100292.
[12] L. Sobotta, P. Skupin-Mrugalska, J. Piskorz, J. Mielcarek, Porphyrinoid photosensitizers mediated photodynamic inactivation against bacteria, Eur. J. Med. Chem. 175 (2019) 72–106, https://doi.org/10.1016/j.ejmech.2019.04.057.
[13] M.L. Agazzi, M.B. Ballatore, A.M. Durantini, E.N. Durantini, A.C. Tomé, BODIPYs in antitumoral and antimicrobial photodynamic therapy: an integrating review, J. Photochem. Photobiol. C Photochem. Rev. 40 (2019) 21–48, https://doi.org/10.1016/j.jphotochemrev.2019.04.001.
[14] A.V. Prakash, F. Yazabak, I. Hovor, F. Nakonechny, O. Kulyk, O. Semenova, A. Bazylevich, G. Gellerman, L. Patsenker, Highly efficient near-IR cyclohexene cyanine photosensitizers for antibacterial photodynamic therapy, Dye. Pigment. 211 (2023) 111053, https://doi.org/10.1016/j.dyepig.2022.111053.
[15] D. Ziental, D.T. Mlynarczyk, B. Czarczynska-Goslinska, K. Lewandowski, L. Sobotta, Photosensitizers mediated photodynamic inactivation against fungi, Nanomaterials 11 (2021) 2883, https://doi.org/10.3390/nano11112883.

[16] M.L. Agazzi, V.A.S. Almodovar, N.S. Gsponer, S. Bertolotti, A.C. Tomé, E. N. Durantini, Diketopyrrolopyrrole-fullerene C60 architectures as highly efficient heavy atom-free photosensitizers: synthesis, photophysical properties and photodynamic activity, Org. Biomol. Chem. 18 (2020) 1449–1461, https://doi.org/10.1039/c9ob02487e.
[17] M.E. Pérez, V.A.S. Almodovar, J.E. Durantini, N.S. Gsponer, A.M. Durantini, A. C. Tomé, E.N. Durantini, Diketopyrrolopyrrole derivatives as photosensitizing agents against Staphylococcus aureus, Photochem. Photobiol. 99 (2023) 1131–1141, https://doi.org/10.1111/php.13741.
[18] D. Bevk, L. Marin, L. Lutsen, D. Vanderzande, W. Maes, Thiazolo[5,4-d]thiazoles-promising building blocks in the synthesis of semiconductors for plastic electronics, RSC Adv. 3 (2013) 11418–11431, https://doi.org/10.1039/c3ra40851e.
[19] Y. Lin, H. Fan, Y. Li, X. Zhan, Thiazole-based organic semiconductors for organic electronics, Adv. Mater. 24 (2012) 3087–3106, https://doi.org/10.1002/adma.201200721.
[20] G. Reginato, M. Calamante, A. Dessì, A. Mordini, M. Peruzzini, L. Zani, Cross-coupling reactions: some applications to the synthesis of thiazolothiazole- and benzobisthiazole-based dyes for new generation solar cells (DSSC), J. Organomet. Chem. 771 (2014) 117–123, https://doi.org/10.1016/j.jorganchem.2014.01.024.
[21] A.F.R. Cerqueira, M.G.P.M.S. Neves, A. Jorge Parola, A.C. Tomé, Pyridin-2-ylthiazolothiazoles – synthesis and photophysical properties, Results Chem. 3 (2021) 100246, https://doi.org/10.1016/j.rechem.2021.100246.
[22] I. Roy, S. Bobbala, J. Zhou, M.T. Nguyen, S.K.M. Nalluri, Y. Wu, D.P. Ferris, E. A. Scott, M.R. Wasielewski, J.F. Stoddart, ExTzBox: a glowing cyclophane for live-cell imaging, J. Am. Chem. Soc. 140 (2018) 7206–7212, https://doi.org/10.1021/jacs.8b03066.
[23] B. Li, X. Lu, Y. Tian, D. Li, Embedding multiphoton active units within metal-organic frameworks for turning on high-order multiphoton excited fluorescence for bioimaging, Angew. Chemie Int. Ed. 61 (2022) 202206755, https://doi.org/10.1002/anie.202206755.
[24] N.A. Sayresmith, A. Saminathan, J.K. Sailer, S.M. Patberg, K. Sandor, Y. Krishnan, M.G. Walter, Photostable voltage-sensitive dyes based on simple, solvatofluorochromic, asymmetric thiazolothiazoles, J. Am. Chem. Soc. 141 (2019) 18780–18790, https://doi.org/10.1021/jacs.9b08959.
[25] V. Kumar, S. Sony, N. Kaur, S.M. Mobin, P. Kaur, K. Singh, Thiazolothiazole based donor-π-acceptor fluorophore: protonation/deprotonation triggered molecular switch, sensing and bio-imaging applications, Anal. Chim. Acta 1206 (2022) 339776, https://doi.org/10.1016/j.aca.2022.339776.
[26] W. Zhang, Q. Feng, Z.S. Wang, G. Zhou, Novel thiazolo[5,4-d]thiazole-based organic dyes for quasi-solid-state dye-sensitized solar cells, Chem. - an Asian J. 8 (2013) 939–946, https://doi.org/10.1002/asia.201201202.
[27] A. Dessì, G. Barozzino Consiglio, M. Calamante, G. Reginato, A. Mordini, M. Peruzzini, M. Taddei, A. Sinicropi, M.L. Parisi, F. Fabrizi De Biani, R. Basosi, R. Mori, M. Spatola, M. Bruzzi, L. Zani, Organic chromophores based on a fused bis-thiazole core and their application in dye-sensitized solar cells, Eur. J. Org. Chem. (2013) 1916–1928, https://doi.org/10.1002/ejoc.201201629.
[28] X. Zhu, C. Tian, T. Jin, J. Wang, S.M. Mahurin, W. Mei, Y. Xiong, J. Hu, X. Feng, H. Liu, S. Dai, Thiazolothiazole-linked porous organic polymers, Chem. Commun. 50 (2014) 15055–15058, https://doi.org/10.1039/c4cc07255c.
[29] G. Reginato, A. Mordini, L. Zani, M. Calamante, A. Dessì, Photoactive compounds based on the thiazolo[5,4-d]thiazole core and their application in organic and hybrid photovoltaics, Eur. J. Org. Chem. 2016 (2016) 233–251, https://doi.org/10.1002/ejoc.201501237.
[30] M. Nazim, S. Ameen, M. Shaheer Akhtar, H.S. Shin, D-Π-A-Π-D type thiazolo[5,4-d]thiazole-core organic chromophore and graphene modified PEDOT:PSS buffer layer for efficient bulk heterojunction organic solar cells, Sol. Energy 171 (2018) 366–373, https://doi.org/10.1016/j.solener.2018.06.087.
[31] A. Dessì, M. Calamante, A. Sinicropi, M.L. Parisi, L. Vesce, P. Mariani, B. Taheri, M. Ciocca, A. Di Carlo, L. Zani, A. Mordini, G. Reginato, Thiazolo[5,4- d]thiazole-based organic sensitizers with improved spectral properties for application in greenhouse-integrated dye-sensitized solar cells, Sustain. Energy Fuels 4 (2020) 2309–2321, https://doi.org/10.1039/D0SE00124D.
[32] Y. Wang, Y. Wang, L. Zhu, H. Liu, J. Fang, X. Guo, F. Liu, Z. Tang, M. Zhang, Y. Li, A novel wide-bandgap small molecule donor for high efficiency all-small-molecule organic solar cells with small non-radiative energy losses, Energy Environ. Sci. 13 (2020) 1309–1317, https://doi.org/10.1039/c9ee04199k.
[33] Z. Zhang, Y.A. Chen, W.Y. Hung, W.F. Tang, Y.H. Hsu, C.L. Chen, F.Y. Meng, P. T. Chou, Control of the reversibility of excited-state intramolecular proton transfer (ESIPT) reaction: host-polarity tuning white organic light emitting diode on a new thiazolo[5,4-d]thiazole ESIPT system, Chem. Mater. 28 (2016) 8815–8824, https://doi.org/10.1021/acs.chemmater.6b04707.
[34] P. Li, X.M. Yin, L.L. Gao, S.L. Yang, Q. Sui, T. Gong, E.Q. Gao, Modulating excitation energy of luminescent metal-organic frameworks for detection of Cr(VI) in water, ACS Appl. Nano Mater. 2 (2019) 4646–4654, https://doi.org/10.1021/acsanm.9b01088.
[35] P. Li, M.Y. Guo, X.M. Yin, L.L. Gao, S.L. Yang, R. Bu, T. Gong, E.Q. Gao, Interpenetration-enabled photochromism and fluorescence photomodulation in a metal-organic framework with the thiazolothiazole extended viologen fluorophore, Inorg. Chem. 58 (2019) 14167–14174, https://doi.org/10.1021/acs.inorgchem.9b02220.
[36] A. Khatun, D.K. Panda, N. Sayresmith, M.G. Walter, S. Saha, Thiazolothiazole-based luminescent metal-organic frameworks with ligand-to-ligand energy transfer and Hg 2+ -sensing capabilities, Inorg. Chem. 58 (2019) 12707–12715, https://doi.org/10.1021/acs.inorgchem.9b01595.
[37] G. Sathiyan, S. Chatterjee, P. Sen, A. Garg, R.K. Gupta, A. Singh, Thiazolothiazole-based fluorescence probe towards detection of copper and iron ions through formation of radical cations, ChemistrySelect 4 (2019) 11718–11725, https://doi.org/10.1002/slct.201902994.
[38] Z. Dikmen, O. Turhan, M. Yaman, V. Bütün, An effective fluorescent optical sensor: thiazolo-thiazole based dye exhibiting anion/cation sensitivities and acidochromism, J. Photochem. Photobiol. A Chem. 419 (2021) 113456, https://doi.org/10.1016/j.jphotochem.2021.113456.
[39] A.F.R. Cerqueira, N.M.M. Moura, M.G.P.M.S. Neves, A. Jorge Parola, A.C. Tomé, Improving the sensing ability of thiazolothiazole derivatives towards metal ions, J. Photochem. Photobiol. A Chem. 451 (2024) 115490, https://doi.org/10.1016/j.jphotochem.2024.115490.
[40] Q. Huang, L. Guo, N. Wang, X. Zhu, S. Jin, B. Tan, Layered thiazolo[5,4- d] thiazole-linked conjugated microporous polymers with heteroatom adoption for efficient photocatalysis application, ACS Appl. Mater. Interfaces. 11 (2019) 15861–15868, https://doi.org/10.1021/acsami.8b21765.
[41] Y. Wang, H. Liu, Q. Pan, N. Ding, C. Yang, Z. Zhang, C. Jia, Z. Li, J. Liu, Y. Zhao, Construction of thiazolo[5,4-d]thiazole-based two-dimensional network for efficient photocatalytic CO2 reduction, ACS Appl. Mater. Interfaces 12 (2020) 46483–46489, https://doi.org/10.1021/acsami.0c12173.
[42] E. Flores, M. Muñoz-Osses, C. Torrent, Y. Vásquez-Martínez, A. Gómez, M. Cortez-San Martin, A. Vega, A.A. Martí, F. Godoy, C. Mascayano, Design, synthesis and biological evaluation of ferrocenyl thiazole and thiazolo[5,4-d]thiazole catechols as inhibitors of 5-hLOX and as antibacterials against Staphylococcus aureus, Struct. Relationship Comput. Stud. Organometall. 39 (2020) 2672–2681, https://doi.org/10.1021/acs.organomet.0c00284.
[43] J.C.J.M.D.S. Menezes, M.A.F. Faustino, K.T. De Oliveira, M.P. Uliana, V.F. Ferreira, S. Hackbarth, B. Röder, T. Teixeira Tasso, T. Furuyama, N. Kobayashi, A.M.S. Silva, M.G.P.M.S. Neves, J.A.S. Cavaleiro, Synthesis of new chlorin e6 trimethyl and protoporphyrin IX dimethyl ester derivatives and their photophysical and electrochemical characterizations, Chem. - A Eur. J. 20 (2014) 13644–13655, https://doi.org/10.1002/chem.201403214.
[44] P.G. Mahajan, N.C. Dige, B.D. Vanjare, C.-H. Kim, S.-Y. Seo, K.H. Lee, Design and synthesis of new porphyrin analogues as potent photosensitizers for photodynamic therapy: spectroscopic approach, J. Fluoresc. 30 (2020) 397–406, https://doi.org/10.1007/s10895-020-02513-2.
[45] N.S. Gsponer, M.L. Agazzi, M.B. Spesia, E.N. Durantini, Approaches to unravel pathways of reactive oxygen species in the photoinactivation of bacteria induced by a dicationic fulleropyrrolidinium derivative, Methods 109 (2016) 167–174, https://doi.org/10.1016/j.ymeth.2016.05.019.
[46] S.C. Santamarina, D.A. Heredia, A.M. Durantini, E.N. Durantini, Antimicrobial photosensitizing material based on conjugated Zn(II) porphyrins, Antibiotics 11 (2022) 91, https://doi.org/10.3390/antibiotics11010091.
[47] M.E. Pérez, J.E. Durantini, E. Reynoso, M.G. Alvarez, M.E. Milanesio, E. N. Durantini, Porphyrin-Schiff base conjugates bearing basic amino groups as antimicrobial phototherapeutic agents, Molecules 26 (2021) 5877, https://doi.org/10.3390/molecules26195877.
[48] S.R. Martínez, Y.B. Palacios, D.A. Heredia, M.L. Agazzi, A.M. Durantini, Phenotypic resistance in photodynamic inactivation unravelled at the single bacterium level, ACS Infect. Dis. 5 (2019) 1624–1633, https://doi.org/10.1021/acsinfecdis.9b00185.
[49] J. Luo, B. Hu, C. Debruler, T.L. Liu, A π-conjugation extended viologen as a two-electron storage anolyte for total organic aqueous redox flow batteries, Angew. Chem. - Int. Ed. 57 (2018) 231–235, https://doi.org/10.1002/anie.201710517.
[50] P. Cheng, Q. Shi, Y. Lin, Y. Li, X. Zhan, Evolved structure of thiazolothiazole based small molecules towards enhanced efficiency in organic solar cells, Org. Electron. 14 (2013) 599–606, https://doi.org/10.1016/j.orgel.2012.11.026.
[51] T. Jia, Z. Peng, Q. Li, T. Zhu, Q. Hou, L. Hou, Synthesis of four-armed triphenylamine-based molecules and their applications in organic solar cells, New J. Chem. 39 (2015) 994–1000, https://doi.org/10.1039/c4nj01537a.
[52] R.C. Knighton, A.J. Hallett, B.M. Kariuki, S.J.A. Pope, A one-step synthesis towards new ligands based on aryl-functionalised thiazolo[5,4-d]thiazole chromophores, Tetrahedron Lett. 51 (2010) 5419–5422, https://doi.org/10.1016/j.tetlet.2010.07.172.
[53] M.R. Pinto, Y. Takahata, T.D.Z. Atvars, Photophysical properties of 2,5-diphenyl-thiazolo[5,4- d]thiazole, J. Photochem. Photobiol. A Chem. 143 (2001) 119–127, https://doi.org/10.1016/S1010-6030(01)00520-2.
[54] B. Valeur, M.N. Berberan-Santos, Molecular Fluorescence, Wiley-VCH Verlag GmbH & Co. KGaA, Weinheim, Germany, 2012. https://doi.org/10.1002/9783527650002.
[55] A.N. Woodward, J.M. Kolesar, S.R. Hall, N.A. Saleh, D.S. Jones, M.G. Walter, Thiazolothiazole fluorophores exhibiting strong fluorescence and viologen-like reversible electrochromism, J. Am. Chem. Soc. 139 (2017) 8467–8473, https://doi.org/10.1021/jacs.7b01005.
[56] N. Shankar, P. Soe, C.C. Tam, Prevalence and risk of acquisition of methicillin-resistant Staphylococcus aureus among households: a systematic review, Int. J. Infect. Dis. 92 (2020) 105–113, https://doi.org/10.1016/j.ijid.2020.01.008.
[57] C. Danne, S. Dramsi, Pili of gram-positive bacteria: roles in host colonization, Res. Microbiol. 163 (2012) 645–658, https://doi.org/10.1016/j.resmic.2012.10.012.
[58] K.O. Duedu, C.E. French, Two-colour fluorescence fluorimetric analysis for direct quantification of bacteria and its application in monitoring bacterial growth in cellulose degradation systems, J. Microbiol. Methods 135 (2017) 85–92, https://doi.org/10.1016/j.mimet.2017.02.006.
[59] I. Guzmán-Soto, C. McTiernan, M. Gonzalez-Gomez, A. Ross, K. Gupta, E. J. Suuronen, T.-F. Mah, M. Griffith, E.I. Alarcon, Mimicking biofilm formation and development: recent progress in in vitro and in vivo biofilm models, Iscience 24 (2021) 102443, https://doi.org/10.1016/j.isci.2021.102443.